Applied Catalysis B: Environmental 117–118 (2012) 346–350

Contents lists available at SciVerse ScienceDirect

Applied Catalysis B: Environmental

journal homepage: www.elsevier.com/locate/apcatb

Selective catalytic oxidation of ammonia to nitrogen over CuO/CNTs: The promoting effect of the defects of CNTs on the catalytic activity and selectivity

Shaoqing Song, Shujuan Jiang*

School of Chemistry, Biology and Material, East China Institute of Technology, Nanchang, Jiangxi Province 330013, PR China

ARTICLE INFO

Article history:
Received 3 November 2011
Received in revised form 5 January 2012
Accepted 28 January 2012
Available online 7 February 2012

Keywords:
CuO/CNTs
Ammonia oxidation
N_2 selectivity
Defects

ABSTRACT

CuO/CNTs were prepared as catalysts for the selective catalytic oxidation of ammonia and demonstrated high catalytic activity and N_2 selectivity. The study results showed that the surface defects of carbon nanotubes (CNTs) could not only activate CuO, but also promote the electron transfer in the catalysis. Thus, along with increasing the defect density of the CNTs, the temperature for the complete ammonia oxidation could be decreased from 235 °C to 189 °C and the corresponding N_2 selectivity increased from 93.8% to 98.7%. Moreover, there was no apparent decrease in the catalytic activity at prolonged reaction time, indicating CuO/CNT catalysts are promising for the selective catalytic oxidation of ammonia.

1. Introduction

Ammonia is a toxic and corrosive gas with a pungent odor, and is potentially harmful to public health. Thus, the abatement of ammonia is becoming an important issue due to the increasing environmental concerns. To meet the economic and ecological demands, the selective catalytic oxidation (SCO) of ammonia to nitrogen and water has attracted considerable interests in recent years [1–4]. Various types of materials have been studied as catalysts for SCO process of ammonia. Precious metals have been used as active catalysts for the ammonia oxidation at the low temperature region, such as Pt [4–7], Pd [7,8], Au [9] and Ag [10,11]. Unfortunately, their N_2 selectivity is relatively poor. Transition metal based catalysts were also used for the ammonia SCO process (e.g. Fe_2O_3 [12–14] and CuO [15–19]). In general, these catalysts showed higher selectivity to nitrogen but operated at temperatures significantly higher than precious metal catalysts. From the viewpoint of potential application, transition metal oxides are promising catalysts for SCO. Thus, how to lower the completed catalytic reaction temperature with transition metal oxides as catalysts would be an urgent problem to be resolved. In order to resolve the problem, we chose suitable supports to activate metal components and lower catalytic reaction temperature.

Among the reported supports, carbon nanotubes (CNTs) are promising supports to improve the activity and selectivity due to their favorable structure and unique properties [20]. Researchers have reported that the confinement in CNTs can active metal components and improve their activity [21,22]. In fact, activities of metal components are not only improved by confinement, but also by the surface structures of CNTs (e.g. the defect structure). Here, CuO nanoparticles (NPs) were supported on the surface of CNTs. We investigated which structure could influence the activity of the CuO components on the surface of CNTs. How the surface structure of CNTs activate the CuO NPs and lower the reaction temperature for the ammonia SCO with high N_2 selectivity were further studied in detail. The study results showed that the surface defects of CNTs could activate CuO and lower the reaction temperature. Consequently, the temperature of 189 °C and N_2 selectivity of 98.7% for the complete ammonia oxidation were achieved on the optimized CuO/CNT catalyst.

2. Experimental

2.1. Treatment of CNTs and preparation of CuO/CNTs

3 g of raw CNTs with a diameter of 10–20 nm (Chengdu Organic Chemicals) was suspended in 150 mL of concentrated HNO_3 (68 wt.%) and refluxed at 80, 100, 120, 140 or 180 °C for 5 h, and then filtrated. The filtrated CNTs were all washed thoroughly with deionized water until the pH was around 7, and then dried at 60 °C for 12 h. Then 0.5 g of the treated CNTs was subsequently added into an aqueous $Cu(CH_3COO)_2$ solution under stirring followed by ultrasonic treatment for 25 min. Then the solvent was evaporated slowly under ambient conditions. The resulting solid mixture was gradually heated to 140 °C in air and kept for 3 h before being heated to 350 °C at a rate of 2 °C/min in He and held there for

* Corresponding author. Tel.: +86 791 83896550; fax: +86 791 83896550.
E-mail address: sjjiang@ecit.edu.cn (S. Jiang).

0926-3373/$ – see front matter
doi:10.1016/j.apcatb.2012.01.030

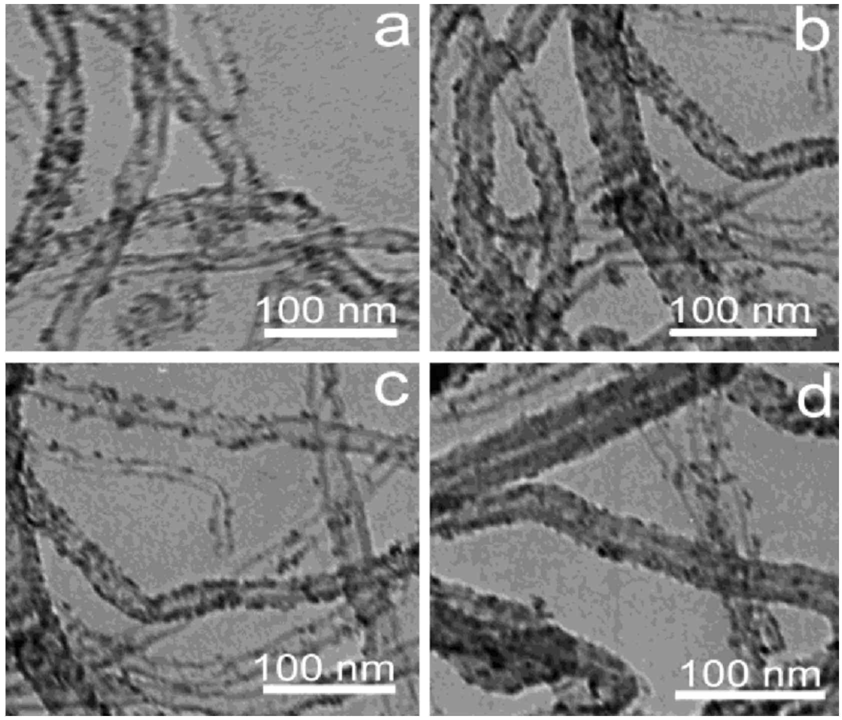

Fig. 1. TEM images of CuO/CNTs. (a) CuO/CNTs-80, (b) CuO/CNTs-100, (c) CuO/CNTs-120 and (d) CuO/CNTs-140. Inserts in (a–d) are the corresponding size distribution histograms of metal nanoparticles for each catalyst based on observation of 300 particles, in which *d* means particle diameter and *F* frequency.

3 h. The prepared nanocomposites were denoted as CuO/CNTs-80, CuO/CNTs-100, CuO/CNTs-120, CuO/CNTs-140 and CuO/CNTs-180 corresponding to the above refluxing temperature of CNTs.

2.2. Characterizations of the prepared samples

The Cu loading amount of samples was analyzed by J-A1100 inductively coupled plasma (ICP, Jarrell-Ash, USA). Transmission electron microscopy (TEM) measurements were carried out with JEOL-JEM-1010 transmission electron microscope at 100 kV. X-ray photoelectron spectroscopy (XPS) was carried out with an ESCALAB 250 electron spectrometer from Thermo of U.S.A. Raman spectra were employed at ambient temperature on a Renishaw inVia Raman Microscope with an argon-ion laser at an excitation wavelength of 514 nm. Temperature-programmed reduction of hydrogen (H_2-TPR) was performed using a flow system equipped with a TCD detector. Typically, 50 mg of the samples was degassed at 100 °C for 1 h with argon gas flow, then cooled to 25 °C, and the gas flow was shifted to a mixture of 5 vol.% H_2 in Ar. The temperature was raised from 25 to 450 °C with a heating temperature rate of 10 °C/min. The water produced during reduction was trapped in a 5A molecular sieve column.

2.3. Catalytic tests

The catalytic reactions for ammonia SCO were performed in a quartz U-type tube microreactor under atmospheric pressure. In the catalytic process, 100 mg of catalyst was placed in the reactor and then suffered thermal treatment at 400 °C for 3 h. When the temperature of the reactor decreased to 135 °C, the reactant gas including 1000 ppm NH_3, 2% O_2 and balance He was fed into the reactor with the flow rate of 100 mL/min. A magnetic deflection type mass spectrometer (AEROVAC^{TM}, Vacuum Technology Inc.) was used to monitor the stream from the reactor including NH_3 (m/e = 17 minus the contribution of H_2O), H_2O (m/e = 18), N_2 (m/e = 28), NO (m/e = 30), O_2 (m/e = 32), N_2O (m/e = 44) and NO_2 (m/e = 46). The products were also analyzed by a gas chromatograph (SP-6890) equipped with a thermal conductivity detector. And 5A molecular sieve column was used to detect N_2 and Porapak Q column for N_2O.

3. Results and discussion

3.1. Characterization of prepared samples

The Cu loadings detected by ICP were about 9.91%, 9.84%, 9.88% and 9.85% for CuO/CNTs-80, CuO/CNTs-100, CuO/CNTs-120 and CuO/CNTs-140, respectively. TEM images shown in Fig. 1 reveal that CuO NPs with average sizes of 7–8 nm were homogeneously dispersed on the surface of CNTs. XPS analysis was used to confirm Cu species on the surface of CNTs. Fig. 2 shows the Cu 2p scan spectrum for each CuO/CNT sample. All the Cu 2p spectra show two

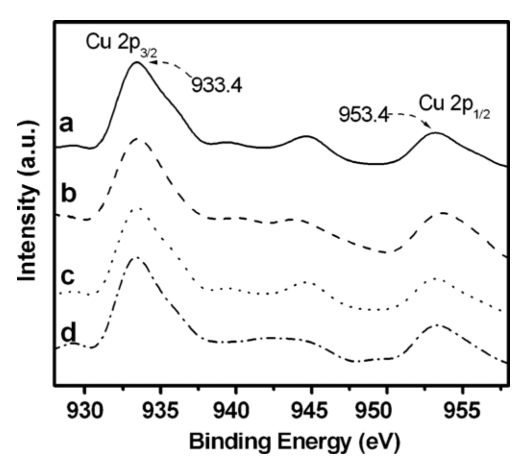

Fig. 2. Cu 2p XPS spectra for CuO/CNTs. (a) CuO/CNTs-80, (b) CuO/CNTs-100, (c) CuO/CNTs-120 and (d) CuO/CNTs-140.

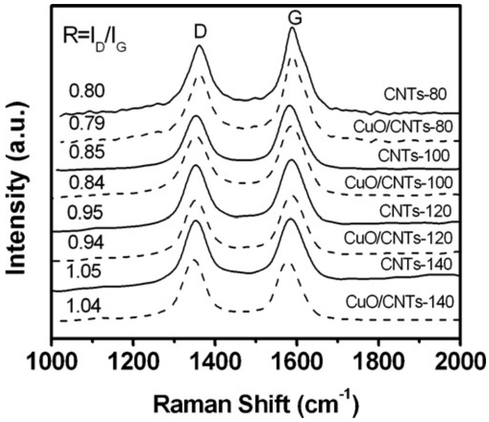

Fig. 3. Raman spectra of the CNTs before and after CuO NPs deposition on CNTs.

main peaks at about 933.4 and 953.4 eV, corresponding to Cu $2p_{3/2}$ and Cu $2p_{1/2}$, which confirms that the Cu species was CuO [23].

3.2. Surface structure characterization

The surface structures of CNTs are composed of perfect graphitize, oxygen-containing groups (—COOH) and defects. The defects including topological defects, incomplete bonding defects, rehybridization defects formed inevitably during the growth of CNTs or modification. For example, the incomplete bonding defects could be formed by destroying the conjugated π-bonds of graphitize in the tube structures of CNTs. It is believed that the defects could not only modify the physical properties but also enhance the chemical reactivity of CNTs. Among these structures, it is reported that metal or metal oxides could be preferentially trapped by the surface defects of CNTs [24], and the formed metal-defect structures can facilitate catalytic reaction [25]. Thus, it is necessary to investigate and confirm the location of the CuO NPs on CNTs. Generally, Raman spectroscopy is often used for determining the deposition site of metal oxides by comparing the defect density of CNTs before and after catalyst preparation [26].

It can be seen that all the four CuO/CNT samples present two main peaks at about 1342 and 1576 cm^{-1} (Fig. 3). The peak around 1342 cm^{-1} (D-band) is associated with the vibrations of carbon atoms in the disordered graphite structure, i.e., the defects. The peak at near 1576 cm^{-1} (G-band) corresponds to the E_{2g} mode of graphite [27]. It is known that the ratio of the intensity of D-bands to G-bands (I_D/I_G) suggests the defect density in CNT samples [28] and here the I_D/I_G is denoted as "*R*". As shown in Fig. 3, *R* is 0.80 for the pristine CNTs-80 and then decreases to 0.79 after CuO loading. The defect densities in CNTs-100, CNTs-120 and CNTs-140 show the same changes after CuO deposition, i.e., the *R* values decrease from 0.85 to 0.84, 0.95 to 0.94 and 1.05 to 1.04, respectively. This means that CuO NPs prefer anchoring onto the defect structures rather than to the perfect sites of CNTs, which is consistent with the study of Banhart and co-workers [24] and Lee and co-workers [26].

3.3. H_2-TPR

The influence of CNTs on the reduction behavior of CuO NPs was investigated by H_2-TPR since the redox behavior and chemical stability of the supported transition metals are essential for applications in catalysis. In Fig. 4b–e, the peaks in the range of 100–300 °C for all samples correspond to the reduction of CuO [29,30], since there is no peak for the reduction of pristine CNTs (Fig. 4a). Fig. 4b shows that CuO NPs supported on CNTs-80 were reduced at 230.2 °C. With increasing the defect density in CNTs, the reduction

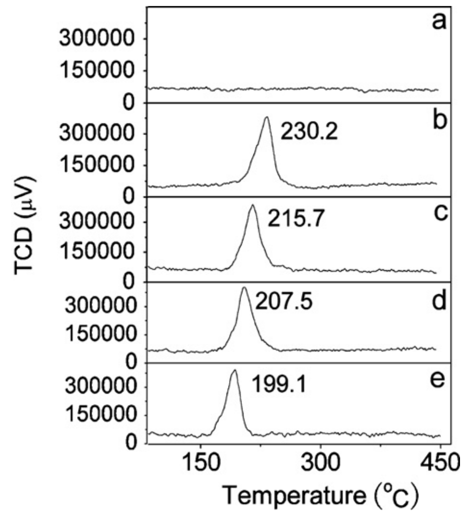

Fig. 4. H_2-TPR profiles of CNTs and CuO/CNTs. (a) pristine CNTs-80, (b) CuO/CNTs-80, (c) CuO/CNTs-100, (d) CuO/CNTs-120 and (e) CuO/CNTs-140.

temperature was stepwise lowered to 215.7 °C (CuO/CNTs-100), 207.5 °C (CuO/CNTs-120) and further down to 199.1 °C (CuO/CNTs-140). Compared with CuO NPs supported on CNTs with highly perfect graphitize structures or CNTs with lots of —COOH groups (S1–3 in Supplementary material), CNTs with high defect density facilitated the reduction of CuO NPs. These results indicate that the reduction temperature of CuO NPs has a strong dependence on the defect density of CNT support. This is attributed to the effect of the defects, because the defects have a profound impact upon electronic transport properties and produce electron acceptor-like states within graphitic materials [31,32]. Thus, the defects could promote electron transfer in the reduction process, which destabilizes the Cu—O bonds and facilitates the reduction of CuO to Cu. The results mean that metal oxides could be activated by the defects on CNTs, which is similar with the effect of the confinement of CNTs [21].

3.4. Catalytic performance

The thermal stability of the catalysts was analyzed by thermogravimetric analysis in air (Fig. S6 in Supplementary material). The weight loss is negligible in all cases below 200–350 °C, increasing particularly from 400 °C in the worst case. This temperature range guarantees the thermal stability of the catalyst during reaction, because our reaction temperature was less than 260 °C.

The catalytic activities of the CuO/CNT catalysts for the ammonia SCO are shown in Fig. 5a. The reaction of NH_3 oxidation on CuO/CNTs-80 started at 135 °C and completed at 235 °C. By increasing the defect density of CNTs, the catalytic activity of CuO/CNTs for NH_3 oxidation was further enhanced. The completed reaction temperature was 217, 206 and 189 °C for CuO/CNTs-100, CuO/CNTs-120 and CuO/CNTs-140 catalyst, respectively. The completed reaction temperature for CuO/CNTs-140 is much lower than those of the reported catalysts [2], which indicated the high catalytic activity of CuO/CNTs for the oxidation of ammonia. Besides the complete ammonia oxidation temperature, the selectivity of NH_3 oxidation to N_2 was also investigated. From Fig. 5b, it can be seen that the N_2 selectivity for the ammonia oxidation on all the CuO/CNTs was above 93.8%, and it even reached 98.7% on CuO/CNTs-140, indicating the promising application of CuO/CNT catalyst for the elimination of ammonia pollution. Moreover, the N_2 selectivity of NH_3 oxidation on the CuO/CNTs increased with increasing defect density of CNTs. This indicates that the defects could not only promote the catalytic activity of CuO/CNTs, but also the N_2 selectivity.

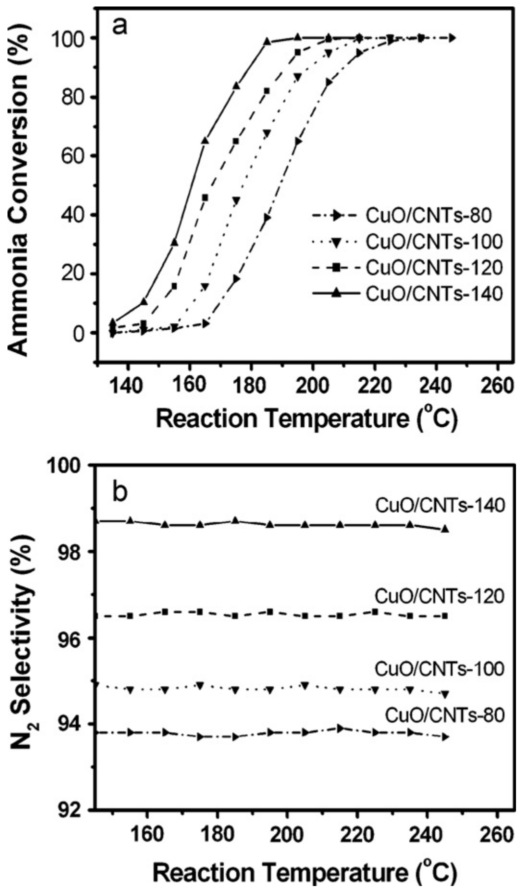

Fig. 5. (a) The catalytic oxidation conversion of NH_3 vs. temperature catalyzed by CuO/CNTs with different defect densities; (b) the corresponding selectivity of NH_3 to N_2 in the catalytic reaction.

Combined with the result of Fig. 4, this should be attributed to two reasons. One reason is that CuO could be activated by the surface defects of CNTs. The other reason is attributed to the facile electron transfer promoted by the defects in catalysis. In the catalytic process, active oxygen is essential for the ammonia SCO, and the electron transfer from the oxygen to CuO promoted by the defects could facilitate the formation of active oxygen. Thus, CuO NPs located on the defect sites of CNTs showed high activity in the ammonia SCO. Moreover, due to their reduction properties [33], the defects can prevent the further oxidation of N_2 to N_2O and/or NO.

Furthermore, the effect of the surface —COOH of CNTs on the catalytic activity and N_2 selectivity was also investigated. CuO/CNTs-100 and CuO/CNTs-180 show almost the same particle sizes, Cu contents and defect density (R = 0.84), but there are more amounts of carboxyl groups in CuO/CNTs-180 than in CuO/CNTs-100 (Figs. S1–4 in Supplementary material). From the catalytic results (Fig. 6), we can see that the completed reaction temperature (231 °C) for CuO/CNTs-180 is higher than that of CuO/CNTs-100 (217 °C), and N_2 selectivity for CuO/CNTs-180 is lower than that of CuO/CNTs-100. The results indicate that the —COOH structure of CNTs can not facilitate catalytic reaction. Moreover, the —COOH groups on CNTs would decrease N_2 selectivity and lead to the over-oxidization of ammonia to N_2O and NO, as shown in Table S1.

Moreover, the stability of CuO/CNTs-140 was tested at a temperature of 189 °C, as shown in Fig. 7. After 15 h on-stream, the conversion of ammonia oxidation was maintained at about 100%. Therefore, CuO/CNT catalyst not only provides high reactivity, but also exhibites good stability, suggesting that CuO/CNTs is a good candidate for ammonia SCO to nitrogen.

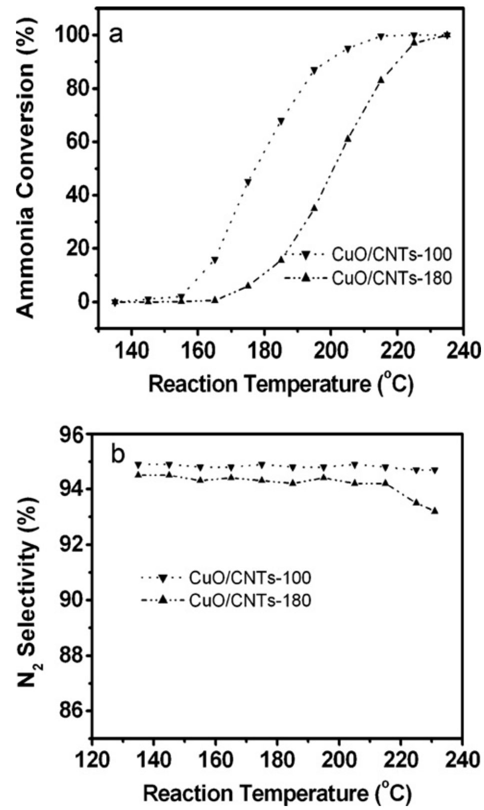

Fig. 6. (a) The catalytic oxidation conversion of NH_3 vs. temperature catalyzed by CuO/CNTs with different —COOH densities; (b) the corresponding selectivity of NH_3 to N_2 in the catalytic reaction.

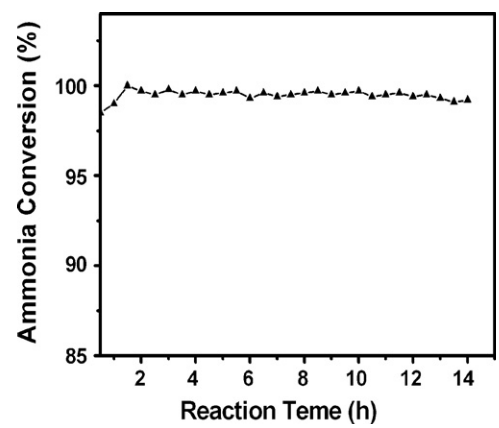

Fig. 7. Time-on-stream behavior of NH_3 oxidation on CuO/CNTs-140 catalyst at a fixed reaction temperature (189 °C).

4. Conclusion

CuO NPs with CNTs as support were used as catalysts for the selective catalytic oxidation of ammonia. The catalytic results showed the temperature for the complete ammonia oxidation was decreased from 235 °C to 189 °C, and the corresponding N_2 selectivity increased from 93.8% to 98.7% by increasing the defect density of CNTs. The good performance of the catalysts mainly arises from (i) CuO could be activated by the surface defects of CNTs, (ii) the electron transfer in the catalysis promoted by the defects. The results indicate that the CuO/CNT catalysts are quite potential for selective catalytic oxidation of ammonia to nitrogen.

Acknowledgments

We gratefully acknowledge the support from the National Natural Science Foundation of China (21103019), the Start-up Fund of the East China Institute of Technology (DHBK1005 and DHBK1009) and the Foundation of Key Laboratory of Radioactive Geology and Exploration Technology Fundamental Science for National Defense (2010RGET15).

Appendix A. Supplementary data

Supplementary data associated with this article can be found, in the online version, at doi:10.1016/j.apcatb.2012.01.030.

References

[1] L. Lietti, G. Ramis, G. Busca, F. Bregani, P. Forzatti, Catal. Today 61 (2000) 187–195.
[2] L. Gang, B.G. Anderson, J. van Grondelle, R.A. van Santen, W.J.H. van Gennip, J.W. Niemantsverdriet, P.J. Kooyman, A. Knoester, H.H. Brongersma, J. Catal. 206 (2002) 60–70.
[3] L. Gang, B.G. Anderson, J. van Grondelle, R.A. van Santen, Appl. Catal. B: Environ. 40 (2003) 101–110.
[4] G. Olofsson, L.R. Wallenberg, A. Andersson, J. Catal. 230 (2005) 1–13.
[5] J. Barbier Jr., L. Oliviero, B. Renard, D. Duprez, Top. Catal. 33 (2005) 77–86.
[6] C.M. Hung, J. Hazard. Mater. 180 (2010) 561–565.
[7] D.J. Cheng, J.H. Lan, D.P. Cao, W.C. Wang, Appl. Catal. B: Environ. 106 (2011) 510–519.
[8] R.Q. Long, R.T. Yang, Catal. Lett. 78 (2002) 353–357.
[9] J.L. Gong, R.A. Ojifinni, T.S. Kim, J.M. White, C.B. Mullins, J. Am. Chem. Soc. 128 (2006) 9012–9013.
[10] L. Zhang, H. He, J. Catal. 268 (2009) 18–25.
[11] L. Zhang, C.B. Zhang, H. He, J. Catal. 261 (2009) 101–109.
[12] R.Q. Long, R.T. Yang, J. Catal. 201 (2001) 145–152.
[13] G.S. Qi, R.T. Yang, Appl. Catal. A: Gen. 287 (2005) 25–33.
[14] A.C. Akah, G. Nkeng, A.A. Garforth, Appl. Catal. B: Environ. 74 (2007) 34–39.
[15] C.M. Hung, Synthesis, Powder Technol. 196 (2009) 56–61.
[16] C.M. Hung, J. Hazard. Mater. 166 (2009) 1314–1320.
[17] L. Chmielarz, P. Kustrowski, M. Drozdek, R. Dziembaj, P. Cool, E.F. Vansant, Catal. Today 114 (2006) 319–325.
[18] X.Z. Cui, J. Zhou, Z.Q. Ye, H.R. Chen, L. Li, M.L. Ruan, J.L. Shi, J. Catal. 270 (2010) 310–317.
[19] A. Kaddouri, N. Dupont, P. Gelin, A. Auroux, Catal. Commun. 15 (2011) 32–36.
[20] D. Tasis, N. Tagmatarchis, A. Bianco, M. Prato, Chem. Rev. 106 (2006) 1105–1136.
[21] W. Chen, Z.L. Fan, X.L. Pan, X.H. Bao, J. Am. Chem. Soc. 130 (2008) 9414–9419.
[22] X.L. Pan, Z.L. Fan, W. Chen, Y.J. Ding, H.Y. Luo, X.H. Bao, Nat. Mater. 6 (2007) 507–511.
[23] G. Avgouropoulos, T. Ioannides, Appl. Catal. A: Gen. 244 (2003) 155–167.
[24] J.A. Rodriguez-Manzo, O. Cretu, F. Banhart, ACS Nano 4 (2010) 3422–3428.
[25] S.Q. Song, S.J. Jiang, H.X. Yang, R.C. Rao, A.M. Zhang, Appl. Catal. A: Gen. 401 (2011) 215–219.
[26] S.J. Kim, Y.J. Park, E.J. Ra, K.K. Kim, K.H. An, Y.H. Lee, J.Y. Choi, C.H. Park, S.K. Doo, M.H. Park, C.W. Yang, Appl. Phys. Lett. 90 (2007) 023114.
[27] C.R. Lin, C.H. Su, C.Y. Chang, C.H. Hung, Y.F. Huang, Surf. Coat. Technol. 200 (2006) 3190–3193.
[28] S.Q. Song, H.X. Yang, R.C. Rao, H.D. Liu, A.M. Zhang, Catal. Commun. 11 (2010) 783–787.
[29] J.Y. Kim, J.A. Rodrguez, J.C. Hanson, A.I. Frenkel, P.L. Lee, J. Am. Chem. Soc. 125 (2003) 10684–10692.
[30] H.Q. Wan, Z. Wang, J. Zhu, X.W. Li, B. Liu, F. Gao, L. Dong, Y. Chen, Appl. Catal. B: Environ. 79 (2008) 254–261.
[31] T. Savage, S. Bhattacharya, B. Sadanadan, J. Gaillard, T.M. Tritt, Y.P. Sun, Y. Wu, S. Nayak, R. Car, N. Marzari, P.M. Ajayan, A.M. Rao, J. Phys.: Condens. Matter 15 (2003) 5915–5921.
[32] A.K. Chakraborty, R.A.J. Woolley, Y.V. Butenko, V.R. Dhanak, L. Siller, M.R.C. Hunt, Carbon 45 (2007) 2744–2750.
[33] S.Q. Song, H.X. Yang, R.C. Rao, H.D. Liu, A.M. Zhang, Appl. Catal. A: Gen. 375 (2010) 265–271.